



OPEN

SUBJECT AREAS:

BIOMEDICAL
ENGINEERING

POLYMERS

Received
6 May 2014Accepted
30 June 2014Published
15 August 2014Correspondence and
requests for materials
should be addressed to
S.-H.L. (dbiomed@
korea.ac.kr)

Self-adhesive epidermal carbon nanotube electronics for tether-free long-term continuous recording of biosignals

Seung Min Lee¹, Hang Jin Byeon², Joong Hoon Lee², Dong Hyun Baek¹, Kwang Ho Lee³, Joung Sook Hong⁴ & Sang-Hoon Lee^{1,5}

¹Department of Biomedical Engineering, College of Health Science, Korea University, Jeongneung 3-dong, Seongbuk-gu, Seoul 136-703, Korea, ²Department of Bio-convergence Engineering, College of Health Science, Korea University, Jeongneung 3-dong, Seongbuk-gu, Seoul 136-703, Korea, ³Department of Advanced Materials Science and Engineering, College of Engineering, Kangwon National University, 1 Kangwondaehak-gil, Chuncheon 200-701, Korea, ⁴Department of Chemical Engineering, Soongsil University, Sangdo-dong, Dongjak-ku, Seoul 156-743, Korea, ⁵KU-KIST Graduate School of Converging of Sciences & Technologies, Korea University, Jeongneung 3-dong, Seongbuk-gu, Seoul 136-703, Korea.

The long-term, continuous, inconspicuous, and noiseless monitoring of bioelectrical signals is critical to the early diagnosis of disease and monitoring health and wellbeing. However, it is a major challenge to record the bioelectrical signals of patients going about their daily lives because of the difficulties of integrating skin-like conducting materials, the measuring system, and medical technologies in a single platform. In this study, we developed a thin epidermis-like electronics that is capable of repeated self-adhesion onto skin, integration with commercial electronic components through soldering, and conformal contact without serious motion artifacts. Using well-mixed carbon nanotubes and adhesive polydimethylsiloxane, we fabricated an epidermal carbon nanotube electronics which maintains excellent conformal contact even within wrinkles in skin, and can be used to record electrocardiogram signals robustly. The electrode is biocompatible and can even be operated in water, which means patients can live normal lives despite wearing a complicated recording system.

Most activities of the human body, such as muscle contraction and movement, nerve function, glandular secretions, heart beating, and brain activity are driven by low levels of electrical current. Therefore, the noiseless and long-term robust measurement at the skin of specific electrical currents (known as biosignals) is critical to obtaining information required for the diagnosis of disease or the monitoring of health. Silver/silver chloride (Ag/AgCl) electrodes have been extensively used to measure biosignals, but are not suitable for long-term monitoring (e.g. Holter monitoring and epilepsy monitoring) because of the degradation of the signal quality due to the drying of the gel over time, skin regrowth, and allergic reactions^{1,2}. To address these problems of Ag/AgCl electrodes, dry surface electrodes have been employed. However, their practical use is limited by the high electrode-to-skin impedance, poor biocompatibility, and high levels of motion artifacts. Recent progress in material science and microtechnology has enabled the development of thin skin-like electronics that conformally laminate onto the surface of the skin and can be used as electrodes³⁻⁶ and sensors⁷⁻¹⁰.

Despite advances in technical integration, the fabrication process of such skin-like electronics is complicated and it is difficult to establish interconnections with conventional electrical devices and to use commercialized electrical components. Although the monitoring of the biosignals of elderly patients is essential to the early diagnosis and prevention of disease, it is difficult to perform the robust recording of biosignals from highly wrinkled and dried skin for a long time with conventional diverse wet and dry electrodes without replacing the electrodes and use of gel. In addition, it is difficult to continue tether-free monitoring of biosignals when patients wearing monitoring system carry out normal activities such as showering or bathing.

In this paper, we present an epidermis-like electronics that can conformally laminate even into the wrinkles of skin, maintain robust contact, and self-adhere onto skin without any additional equipment (such as a belt, tape, or helmet)^{1,3,11,12}, processing or adhesive glue, which can discomfort users and/or cause skin irritations. In contrast to



other electrodes, the metal layer is not in direct contact with the surface of the skin and commercial electronic components can be easily integrated by general soldering method. For the engineering of such electronics, we hypothesized that a well-dispersed mixture of adhesive polydimethylsiloxane (aPDMS) having excellent biocompatibility and mechanical property, and multi-walled carbon-nanotubes (CNTs) which have excellent electrical conductivity^{13–15} may provide enhanced conformal contact, self-adhesion, biocompatibility and excellent contact impedance. In previous studies, it has been shown that mixing PDMS with conductive materials such as silver microspheres, silver nanowires and CNTs yields a flexible, stretchable, and yet conductive polymer^{16–18}. Among these conductive materials, silver microspheres and silver nanowires are more conductive compared to the CNTs. However, the silver microspheres require much higher concentration in mix with PDMS, as they are easily non-contacted when the polymer is stretched or bent. The silver nanowires has a linear geometry, which makes it less flexible, and can also induce less contact with each other when polymer is bent or stretched. On the other hand, the CNTs are tangled, and assembled randomly, which allows it to have a better contact with each other even when the polymer is bent or stretched. Moreover, the CNTs are inexpensive and highly accessible. Therefore, the CNTs are a better candidate than the silver microspheres or silver nanowires for application in conductive polymer as biosignal-electrode. However, well-mixing of both materials enough to have good conductivity is difficult, and we developed the mixing method. The fabricated CNT/aPDMS electronics is sufficiently thin and flexible to be compatible with the mechanical properties of the skin, and its modulus is comparable to that of epidermis. By using the proposed technology, we fabricated a self-adhesive electrode that can record various biosignals including electrocardiograms (ECGs), electrooculograms (EOGs), and electromyograms (EMGs) without damaging the skin. To demonstrate its usefulness in the inconspicuous monitoring of signals, we developed a self-adhesive and long-term wearable epidermis-like ECG patch, on which measurement and wireless communication system is integrated. It showed excellent performance in ubiquitous long-term recording of ECG signals. Furthermore, its noise and motion artifacts are comparable to those of commercial Ag/AgCl electrodes. The proposed technology enables the unconscious continuous monitoring of personal health regardless of a patient's location and activity and maximizes patient autonomy, which means that it will have extensive applications in biomedical areas and other industry including game, robotics and diverse mobile and wearable devices.

Result

Fabrication of the ECG patch. The main goal of this study was to fabricate an interfacial layer that is conductive, self-adhesive, and thin, and that provides ultra-conformal contact with the skin; such a layer was achieved by well-dispersed mixing of CNTs in aPDMS (MG7-9850, Dow Chemical Corp.). CNTs have high conductivity, so were used to fabricate the conductive interfacial layer through their thorough dispersion in aPDMS with a wetting and flow stress process (Fig. 1a). Then, the dispersed CNTs are in electrical contact each other and CNT/aPDMS becomes conductive. A scanning electron microscopy (SEM) image of the well-dispersed CNTs in CNT/aPDMS is shown in Fig. 1b. By covering a metal-patterned polyimide (PI) electrode with CNT/aPDMS layer, the epidermal CNT-based electrode was fabricated. Due to the softness and adhesiveness of the CNT/aPDMS layer, it penetrates the wrinkles of the epidermis and maintains robust contact (Fig. 1c). Fig. 1d and Supplementary Fig. S1 show a SEM image of a CNT/aPDMS layer and a human skin replica (Supplementary Fig. S2). As suggested by Fig. 1c, the CNT/aPDMS layer is in conformal contact even with wrinkled and rough skin.

We fabricated a self-adhesive ECG patch with this CNT/aPDMS layer (Fig. 1e). The base PDMS layer and metal-patterned PI layer was fabricated and bonded; the CNT/aPDMS layer was bonded onto the top (metal patterned side) of the PI layer, and then, the electrode face was covered with an aPDMS frame layer. The metal-patterned PI layer is completely encapsulated by the CNT/aPDMS, frame, and base layers. The overall shape of the electrode is that of an equilateral triangle. Three ECG lead-electrodes (ELEs) covered with CNT/aPDMS were placed at each corner in the position of right arm (RA), left arm (LA), and left leg (LL), as in the standard ECG recording method. The rest of the electrode was covered with CNT/aPDMS-based driven-right-leg (DRL) electrodes to enhance signal quality through the active noise canceling technique. Top and bottom optical images of the electrode are shown in Figs. 1f and g. To connect the ELE and DRL electrodes to external measurement systems, four terminals are located at the center of the ECG patch. Each ELE and DRL are interconnected with serpentine lines to enhance the flexibility and stretchability of the electrode^{19,20}. The thicknesses of the base layer, PI layer, and CNT/aPDMS layer are 20 μm , 10 μm , and about 90 μm respectively and the CNT/aPDMS layer maintained excellent conformal contact regardless of skin surface (Fig. 1d and Supplementary Fig. S1).

Mechanical property test. An aPDMS, in which the methyl group of PDMS is replaced with a vinyl group ($\text{CH}_2=\text{CH}-$), exhibits light crosslinking to functionalized polydiorganosiloxane, which can be used as a skin adhesive substance and has a weak modulus compared to that of a typical gelled PDMS elastomer²¹. For this purpose, we used MG 7-9850 which is U.S. FDA approved. It is composed of two platinum-catalyzed elastomeric PDMSs (MG 7-9850A and MG 7-9850B) and has medium adhesiveness among the aPDMS series. This adhesive force enables the gentle removal of the electrode without serious skin trauma. However, well-dispersion of CNTs in a viscous aPDMS solution is difficult because CNTs remain as entangled aggregates due to van der Waals attraction. For facile dispersion, we dispersed the CNTs by using the solvent-wet dispersion method²². The additional wetting of the dry CNTs reduces their surface energy without any chemical modification and makes dispersion in a viscous fluid much easier. The solvent-wet dispersion of the CNTs was performed in two steps (Supplementary Fig. S3). First, the CNTs were wetted in solvent (Ethanol) prior to dispersion in aPDMS. Second, the solvent-wet CNTs were mixed with MG 7-9850A (5 wt%) under intensive shear flow by using a home-made stirrer (250 rpm, diameter of cylindrical stirrer = 5.5 cm, gap between the beaker and cylindrical stirrer = 1 mm) for 15 h. Under intensive shear flow, hydrodynamic energy is transferred to the aggregated solvent-wet CNTs to produce dispersion (Step II). The CNT-dispersed MG 7-9850A is mixed with MG 7-9850B and cured to generate the gelled CNT/aPDMS. To confirm whether the CNTs are well dispersed in aPDMS, the CNT/aPDMS was observed through SEM. Prior to observation, the fractured surface of CNT/aPDMS was exposed in tetrahydrofuran (THF, Sigma-Aldrich) solution for 5 h, to enhance observation. A SEM image of the CNT/aPDMS is shown in Fig. 1b: CNTs are homogeneously embedded in aPDMS with no empty spaces because aPDMS successfully diffuses into the CNT clusters. The material properties of CNT/aPDMS were investigated by comparing its Fourier transform infrared spectroscopy (FTIR) spectrum to that of aPDMS. The spectra are indistinguishable (Supplementary Fig. S4a), which indicates that mixing the CNTs into aPDMS does not change the molecular structure of aPDMS. The contact angle of aPDMS and CNT/aPDMS is 122° and 116°, which is almost similar (Supplementary Fig. S4b and S4c).

To quantify the adhesion properties of CNT/aPDMS, we performed adhesion tests and measured the adhesive force of the electrode with a force meter (FGN-5B, NIDEC-SHIMPO Corp.)^{23,24}.

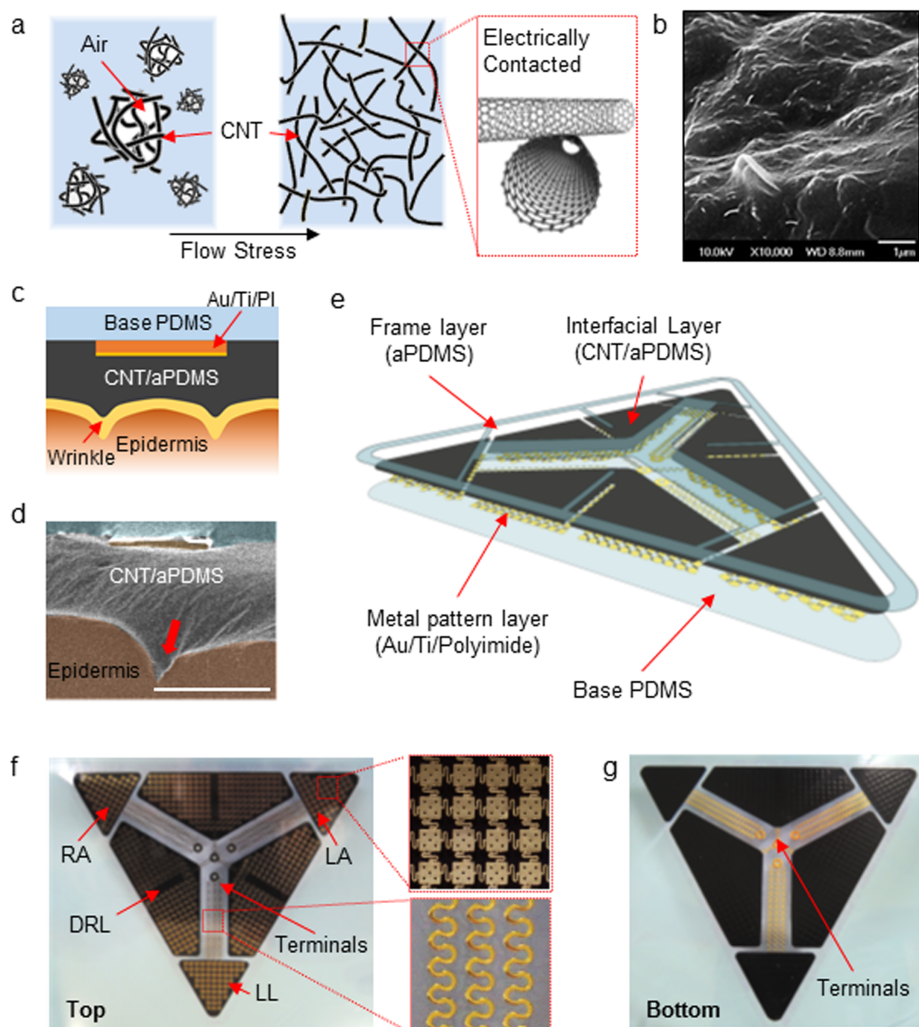


Figure 1 | ECG electrode based on CNT/aPDMS. (a) The aggregated CNTs are mixed with aPDMS by using flow stress. The CNTs are in electrical contact, which means that CNT/aPDMS is conductive. (b) A SEM image of CNT/aPDMS after removal of some aPDMS with THF solution. (c) Conformal contact of CNT/aPDMS with wrinkles and rough skin and (d) a SEM image of a CNT/aPDMS electrode attached to a PDMS skin replica. (e) Structure of an ECG electrode composed of a PDMS base, a metal-patterned layer (Au/Ti/PI), a frame layer (aPDMS), and a CNT/aPDMS interfacial layer. (f) Upper surface of the ECG electrode and serpentine lines. (g) Bottom surface of the ECG electrode, which is the surface attached to the chest.

When CNT/aPDMS is attached to skin, its adhesive force is 1.1 N/cm^2 , which is sufficiently strong for skin attachment, as shown in Fig. 2a. We repeated attach/detach testing and cleaned the surface of CNT/aPDMS with methanol every five cycles. Fig. 2b shows the results of the adhesion tests: as attach/detach is repeated, the adhesion force gradually decreases. After cleaning, the adhesive force recovers but is slightly lower, 1.0 N/cm^2 . The Young's modulus of CNT/aPDMS was also measured using an Instron Model 5567 (TestResources, Shakopee) (Fig. 2c). It was found that CNT/aPDMS has much lower modulus (27.5 kPa) than PDMS ($\sim 1 \text{ MPa}$); this value is comparable to that of skin (130 kPa)^{25,26}. This low modulus enhances the mechanical matching of the large electrode to soft skin and increases its ability to penetrate skin wrinkles. To quantify and investigate the level of conformal contact with skin, we prepared a PDMS skin replica³ (Supplementary Fig. S2). Fig. 2d shows a SEM image of the PDMS skin replica. The surface of the skin replica contains wrinkles. The PDMS skin replica is transparent, so the contact of the skin replica with the CNT/aPDMS electrode can be examined from beneath (Fig. 2e). We attached CNT/aPDMS to the skin replica to determine the degree of contact of the electrode with the skin surface. Where a black substrate is not in close contact with the surface, the non-contacted area appears gray due to the air gap, whereas it appears completely black when in

conformal contact. We determined the contact area of the CNT/aPDMS electrode, commercialized black tape (Temflex 1711, 3M) and a CNT/PDMS²² sheet respectively. Optical images of the contact surfaces are shown in Figs. 2f–h. As CNT/PDMS are rigid and not adhesive, its contacted area was quite small so pressure (15 N/cm^2) was applied. We measured the fraction of contact area by using the expression (area of black color)/(total area), and found values for the black tape, CNT/PDMS, and CNT/aPDMS of 30.9%, 61.9%, and 99.7% respectively.

The contact area of CNT/aPDMS is almost 100%, which means that it almost completely covers the skin replica, even the narrow wrinkles. For more quantitative test, we tested the penetration of CNT/aPDMS into sharp triangular, circle and bar shaped grooves (depth = $50 \mu\text{m}$) engraved on PDMS substrate (Supplementary Fig. S5). As a result, the CNT/aPDMS fully penetrated into the grooves indicating the excellent conformal contact. This ultra-high conformal contact means that the large electrode can be stably attached to curved and wrinkled skin while maintaining excellent contact impedance and robustness with respect to motion artifacts and noise^{27,28}.

Electric property measurements. The impedance from the heart to the amplifier is composed of the impedance between the heart and

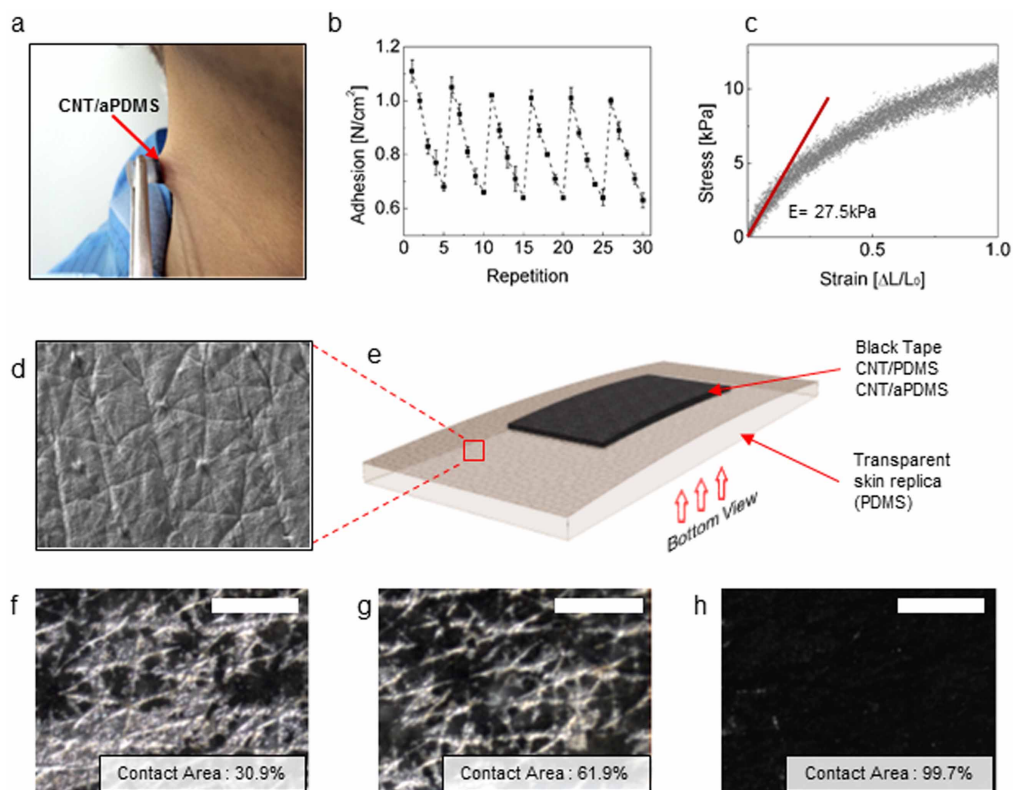


Figure 2 | Adhesiveness and penetrative properties of CNT/aPDMS. (a) The adhesiveness of CNT/aPDMS. (b) Adhesion force measurements during repeated attaching and detaching processes. The CNT/aPDMS surface was cleaned every five cycles. (c) The Young's modulus of CNT/aPDMS. The modulus was calculated to be 27.5 kPa. (d) SEM image of the PDMS skin replica. (e) Black tape, CNT/PDMS, and CNT/aPDMS were attached to the skin replica to determine their contact areas. Images of the contact areas on (f) black tape, (g) CNT/PDMS, and (h) CNT/aPDMS; the percentage contact areas were calculated to be 30.9%, 61.9%, and 99.7% respectively. (scale bar: 3 mm, pressure was applied to CNT/PDMS).

the epidermis (Z_{HE}), the contact impedance between CNT/aPDMS and the epidermis (Z_{CE}), the intrinsic impedance of CNT/aPDMS (Z_C), and the contact impedance between CNT/aPDMS and the metal-patterned layer (Z_{CM}), as shown in Fig. 3a. We measured Z_C and Z_{CM} for various concentrations of CNTs (1.0, 1.5, 2.0, and 2.5 wt%) by using the Solartron 1260 impedance spectroscopy system (ISS) (Supplementary Figs. S6a and b). Z_C is almost constant for all frequencies and is resistive and the conductivity of Z_C are shown for the various concentrations of CNTs in Fig. 3b. As the concentration of CNTs increases, the conductivity increases to a value of 16.4 S/m for a CNT concentration of 2.5 wt%. Z_{CM} decreases to 2.2 k Ω as the CNT concentration increases (Fig. 3c). For comparison, we prepared a dry electrode (without CNT/aPDMS) and an Ag/AgCl electrode (Meditrace 100, Kendall) and Z_{CE} of them were measured after attaching on the left arm and analyzed (Supplementary Figs. S6c and d). The Z_{CE} of the dry electrode was found to be 1.5 M Ω at 40 Hz (Fig. 3d). In contrast, the Z_{CE} of the CNT/aPDMS electrode is approximately 241 k Ω at 40 Hz and that of the Ag/AgCl electrode with gel is 74.2 k Ω at 40 Hz. When the CNT/aPDMS was stretched, the Z_C value was increased as shown in Supplementary Fig. S7a. Moreover, this increased impedance was not restored if it was once stretched at 30% (Supplementary Fig. S7b). Meanwhile, the Z_C value was maintained while the tensile strain was repeated. This is because the electrically contacted CNTs lost the contact with each other when the strain force was applied, and did not revert to the original status. However, the Z_C value is relatively insignificant compared to other impedances, and the thickness of CNT/aPDMS seldom varies, as it is unlikely to be any strain force in vertical direction when the electrode is attached on the skin. Therefore, the change in the Z_C value will not significantly affect the performance of the electrode.

Although CNT/aPDMS provides close contact with skin and has low contact impedance, its robustness with respect to motion artifacts also needs to be considered. Motion artifacts arise especially when a subject stretches the epidermis with various body motions²⁹. When the epidermis stretches but the electrode does not, the change in the contact impedance generates a motion artifact. In addition, body motions jerk the connection line between the electrode and the measurement system, which means that the contact impedance varies abruptly. We anticipated that since CNT/aPDMS has a low Young's modulus and its impedance is robust with respect to stretching, it could easily adapt to body motion without a significant change in its impedance. We determined the stretching ratio of a subject's skin by marking dots on their left chest at intervals of 2 cm and then measuring the changes in their positions as the subject moved their arms in four directions: upward, to the side, forward, and backward (Supplementary Fig. S8). The degree of stretching was determined and it was found that the chest skin stretches by up to 30%. To maintain conformal contact of the electrode with the skin under strain stress, we designed a lead electrode consisting of 1 mm square pieces in length, as shown in Supplementary Fig. S9a. Each square was connected with serpentines (width = 100 μm , $r_{\text{inner}} = 75 \mu\text{m}$, $r_{\text{outer}} = 125 \mu\text{m}$) and a serpentine line from ELE to terminal was also designed (see Supplementary Fig. S9b) that accommodates stretching. Optical images of the serpentine interconnections under mechanical stretches of up to 30% along the x-direction are shown in Supplementary Figs. S9c and d; no mechanical fractures were observed. To quantify motion artifacts and evaluate motion tolerance, two CNT/aPDMS electrodes with serpentine line were attached 4 cm apart (center to center) to the left arm of a subject (Fig. 4a). Conventional Ag/AgCl electrodes and dry electrodes with serpentine line were also tested on the left arm for comparison. We

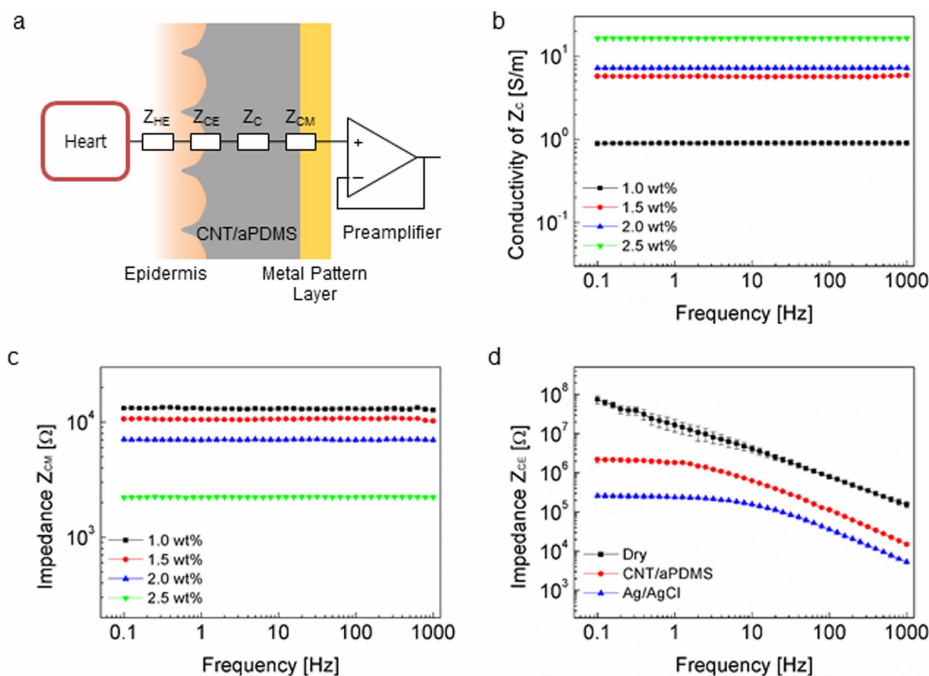


Figure 3 | Electrical properties of CNT/aPDMS. (a) Schematic diagram of the impedance from the heart to the preamplifier, which is composed of the impedance from the heart to the epidermis (Z_{HE}), the contact impedance between CNT/aPDMS and the epidermis (Z_{CE}), the intrinsic impedance of CNT/aPDMS (Z_C), and the contact impedance between CNT/aPDMS and the metal-patterned layer (Z_{CM}). (b) The conductivity of Z_C increases as the concentration of CNTs increases. (c) Z_{CM} is also resistive and its impedance decreases with the concentration of CNTs. (d) Z_{CE} is much higher than the other impedances between the heart and the amplifier. The impedance of the dry electrode is the highest and that of the Ag/AgCl electrode is the lowest.

placed the left arm on an orbital shaker that rotates in a circle ($d=3$ cm) with a variable frequency of motion. Each electrode was connected to a bio-potential measurement system (MP150, Biopac Systems, Inc.). The rotating frequency of the shaker was adjusted to 1, 2, or 3 Hz and the motion artifacts of the dry, Ag/AgCl, and CNT/aPDMS electrodes were recorded (Fig. 4b). We quantified the motion artifacts by calculating their root-mean-square (RMS) values. The RMS of the dry electrode increased from 7.7 to 222.9 mV (saturated signal) as the frequency was increased from 1 to 3 Hz, whereas the RMS variation of the CNT/aPDMS electrode was 4.7 ~ 49.9 mV, and that of the Ag/AgCl electrode was 2.0 ~ 61.4 mV (Fig. 4c). At 3 Hz, the artifact of the CNT/aPDMS electrode is smaller than that of the Ag/AgCl electrode. This result can be explained as follows: although its contact impedance is greater than that of the Ag/AgCl electrode, the softness and conformal contact of the CNT/aPDMS electrode means that it can absorb some of the effects of these motions. The dry electrode has the highest contact impedance of the tested electrodes and as a result its signal was saturated at 3 Hz even though serpentine metal patterns were adopted.

Solderable interface. Most available electronic components are not suitable for use with stretchable and flexible electrode, which would narrow its applications. In order to embed an electronic system in the electrode and enable facile connection to an external system via soldering, we performed Ni electroplating³⁰. By using a punch ($d=1.5$ mm), we produced a hole at the center of each terminal, then Ni electroplating was performed (Supplementary Fig. S10a) to build an anchor for soldering. The Ni-elastomer interconnection is strong because the electroplated Ni adheres strongly to the area around the hole. To connect the preamplifier to the electrode for enhancement in signal quality, we designed a commercialized flexible printed circuit board (FPCB), as shown in Supplementary Fig. S10b. A preamplifier (AD8643, Analog Devices Inc.) and commercialized electrical lines were soldered to this board. The FPCB was designed with four holes for connections to the

terminals of the ECG patch. The four holes in the FPCB were covered with copper and then electroplated with Au on both sides and electrically connected. Once the FPCB had been soldered to the terminals of the ECG patch (Supplementary Fig. S10c), the biopotential measurement system was robustly connected to the ECG patch.

ECG measurements. To measure ECGs, we customized an ECG acquisition module. As shown in Supplementary Figs. S11a and b, the signals from the three preamplifiers pass to an instrument amplifier (INA118, Burr-Brown Co.), and then are high-pass filtered ($f_c = 0.5$ Hz, 2nd order, Butterworth) to eliminate offsets and fluctuations. These signals are amplified and low-pass filtered ($f_c = 40$ Hz, 4th order, Butterworth) to reduce external noise such as that due to power lines. For the DRL, the summed RA and LA signals of the ECG were amplified with a -10 V/V gain. The ECG signals were digitized and sampled with a 1 kHz by 16 bit analog-to-digital converter (AD974, Analog Devices Inc.) and were transmitted to a microprocessor (ATmega128, Atmel Corp.).

To ensure that the electrode is tether-free, we adopted a Bluetooth wireless communication system that can transmit ECG data without cables. To record the ECG data via Bluetooth, we implemented a customized ECG acquisition program on a notebook by using Visual Studio 2007 (Supplementary Fig. S11c). The ECG data from the ECG acquisition module was received with a USB-type Bluetooth dongle (Supplementary Fig. S11d) and displayed on the screen. Further, a real-time software low pass filter with a 45 Hz cutoff frequency (71st order, finite impulse response filter) was implemented in the ECG acquisition program to remove external noise once more. For feasibility testing, we attached the ECG patch to the left chest of a subject, as shown in Fig. 4d. The developed electrode was placed in conformal contact with the skin and attached very reliably to the surface of the chest (Fig. 4e). For comparison, dry and Ag/AgCl electrodes with the same locations at the RA, LA, and LL positions of the ECG patch were also tested. As the dry electrode does not have

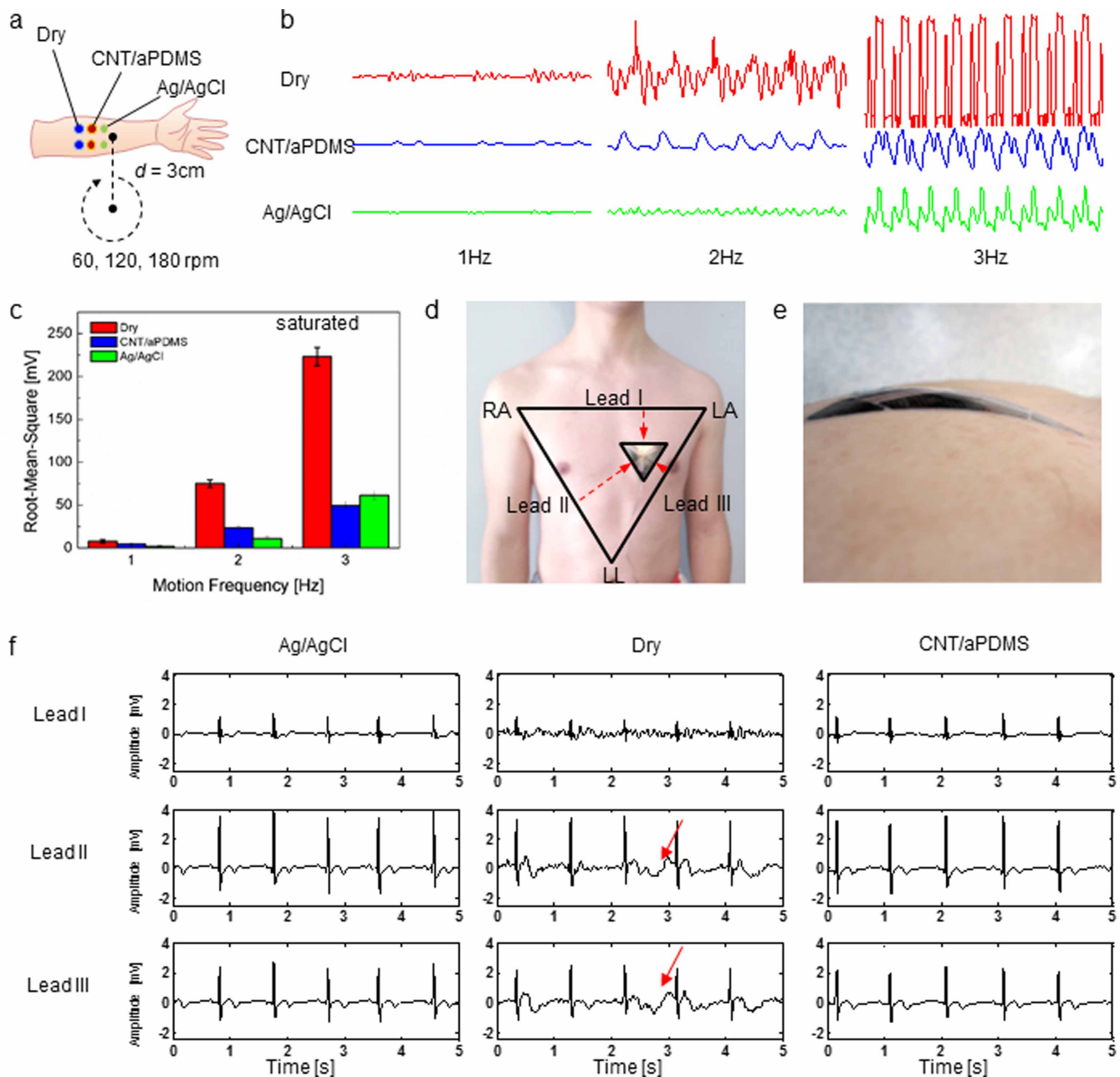


Figure 4 | Motion artifact tests and ECG measurements. (a) Experimental set-up for motion artifact testing. Dry, CNT/aPDMS, and Ag/AgCl electrodes were attached to the left arm in separate tests. In each test, the arm was placed on the shaker, which rotates in a circle ($d=3$ cm) with a frequency of 60, 120, or 180 rpm; these frequencies correspond to the 1, 2, and 3 Hz motion artifacts respectively. (b) Recorded motion artifacts for dry, CNT/aPDMS and Ag/AgCl electrodes for motions with frequencies of 1, 2, and 3 Hz and (c) their RMS values. (d) Attachment of the ECG electrode to the left chest. Triangle shaped RA, LA and LL electrodes represent leads I, II and III. (e) The thin and flexible ECG electrode was robustly attached. (f) ECG waveforms recorded with leads I, II, and III for the Ag/AgCl, dry, and CNT/aPDMS electrodes. The waveforms of CNT/aPDMS are comparable to those of the Ag/AgCl electrode whereas noise and artifacts (arrow) are evident in the signals of the dry electrode.

adhesive properties, it was affixed with air-permeable surgical tape (1533-1, 3M). The ECGs recorded with these electrodes are shown in Fig. 4f. The ECGs from the Ag/AgCl and CNT/aPDMS electrodes are very clear and similar. In contrast, the ECG from the dry electrode is noisy and the baseline is not reliable because drifts are evident. The CNT/aPDMS electrode produces clear and reliable ECG signals that are comparable to those of the commercial Ag/AgCl electrode even though it does not use gel. This tendency was dominantly observed when the distance between a couple of electrodes was reduced. When the distance was reduced to 2 cm, ECG amplitude from three different types were reduced as shown in Supplementary Fig. S12a. Although the dry electrodes showed an unstable and noisy ECG

waveform, the CNT/aPDMS electrodes exhibited a relatively clear and reliable ECG waveform, even when compared to those of the Ag/AgCl electrodes. We also tested the multiple peel-off process by repeatedly attaching and detaching the electrodes for 30 times without a cleaning procedure, but we did not find any difference in ECG waveform as shown in Supplementary Fig. S12b. This implies that the contact impedance was not significantly affected although there was a decrease in adhesion force during the attaching and detaching procedure (Fig. 2b).

To evaluate the waveform accuracy of the ECG patch, we built an artificial chest with agarose gel and an ECG simulator (TMS3000, TRISMED) (Fig. S13a). We compared the signals recorded with the

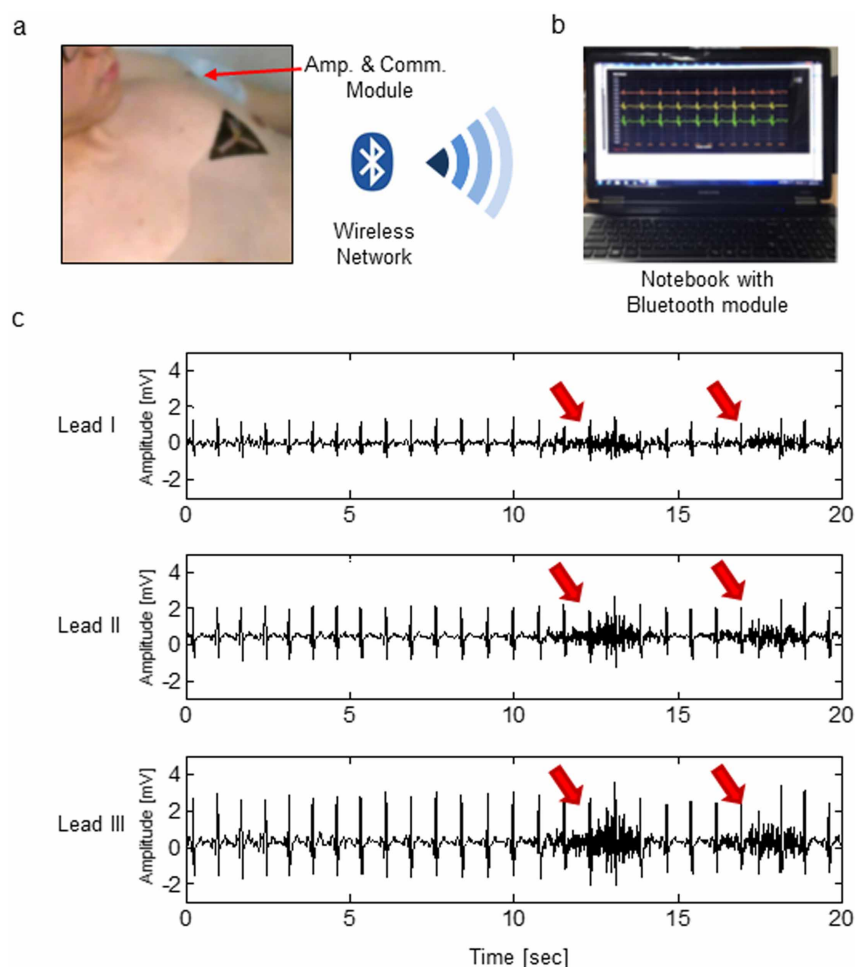


Figure 5 | ECG measurements in watery environments. (a) The ECG electrode remains robustly attached to the chest even when the electrode is submerged in bath water. The ECG acquisition module was affixed to the left arm with an elastic band and a Bluetooth communication system transmitted the ECG signal to a (b) distant notebook wirelessly. (c) The ECG waveform recorded during the bath. An EMG signal (arrows) arose intermittently when the subject changed his body posture.

Ag/AgCl and CNT/aPDMS electrodes. No differences are evident between the results obtained with these two electrodes, and the correlations of the measured signal were 0.998, 0.997, and 0.998 for simulated ECGs of leads I, II, and III respectively (Supplementary Fig. S13b).

The ECG patch is also fully waterproof because the metal-patterned layer is encapsulated with PDMS, aPDMS and CNT/aPDMS. To confirm that the patch is waterproof, we attached part of an ECG patch to the forearm (Fig. S14a) and stained it with blue-colored water. After rubbing the electrode with a finger several times, we removed colored water by using a tissue and then the electrode was peeled off (Video S1). It can be seen in Fig. S14b that the water did not penetrate the area in contact with the electrode. If the electrode was not in close and conformal contact with the skin, the water would penetrate into the gap between the electrode and skin and the electrode would be detached (Supplementary Fig. S14c). The surface of the ECG patch, however, is not only hydrophobic but also penetrates into the wrinkles and is robustly attached to the skin. As a result, water cannot penetrate into the gap between the ECG patch and the skin; thus the subject can take a shower or get into a water-filled bath while their ECG signals are monitored. We confirmed the feasibility of the electrode by recording ECGs even when the electrode was submerged in a water-filled bath (Fig. 5a). To protect the ECG acquisition and wireless communication circuits from the water, we placed them into a waterproof plastic box with two coin batteries and affixed the box to the subject's left arm

band. The ECG acquisition module transmits ECG signals using wireless communication, so the subject could freely move around the house while ECG was monitored (Fig. 5b). The connection cable was bonded to the CNT/aPDMS electrode by soldering, and FPCB was sealed. Wearing the tether-free ECG monitoring system, the subject entered the bath, and no effects on the signal of water or motion artifacts were observed (Fig. 5c, Video S2). EMG signals appeared only when the subject used the muscles of the chest such as during changes in posture. The ECG was successfully recorded with the wireless communication system even when the electrode and the system were fully submerged in water.

Cytotoxicity and skin compatibility tests. The cytotoxicity of CNT/aPDMS was tested by culturing human fibroblast cells (CCD-986Sk) on CNT/aPDMS. After washing the cells with phosphate-buffered saline, they were detached from the flask. A total of 1×10^5 cells were seeded and cultured for a week in Dulbecco's Modified Eagle Medium (Gibco BRL, Life Technologies, Inc.) with high glucose supplementation, 10% fetal bovine serum (Gibco) and 1% antibiotics containing 10,000 units of penicillin and streptomycin (Gibco), at 37°C in a humidified 5% CO₂ environment. The cytotoxicity was evaluated with an Invitrogen Live/Dead Assay Kit. As a result, most cells were uniformly spread on the surface of CNT/aPDMS maintaining their viability, which indicates that CNT/aPDMS does not toxic to cells (Supplementary Fig. S15a). The viability of mouse fibroblast L929 cells on CNT/aPDMS was also



measured using Cell Counting Kit-8 (CCK-8; Dojindo Laboratories, Tabaru, Japan) according to the manufacturer's instructions. The cells were also cultured on aPDMS as a control group. After culturing the cells for 1, 3, and 7 days, the cell numbers increased 174% on day 3, and 1191% on day 7 for CNT/aPDMS; on aPDMS, the cell numbers increased 223% on day 3, and 1518% on day 7 (Supplementary Fig. S15b). On day 7, the viability of the cells on CNT/aPDMS remained 80%, compared to that of the cells on aPDMS. From these results, we conclude that the fibroblast cells highly proliferated on both aPDMS and CNT/aPDMS surfaces and also that CNT/aPDMS would be biocompatible. The CNT/aPDMS electrode was also continuously attached to the chest of a subject for a week to evaluate its skin compatibility. After a week, the skin where the electrode had been attached was normal and no itching or erythema was found (Supplementary Fig. S15c). On the other hand, as time passed by, the dead cells from the surface of the skin exfoliated and this resulted in reduced ECG amplitude as shown in Supplementary Fig. S16. However, the ECG waveform was still in high quality; and moreover, its amplitude was restored after a cleaning process.

Discussion

Inconspicuous continuous and robust monitoring of personal health with a skin-like system has long been a dream of humanity, and the proposed CNT/aPDMS electronics could realize this dream. The thickness of the electronics (ECG patch) is 120 μm and it is flexible, biocompatible, and stretchable. This electronics is self-adhesive and conformal contact is maintained even in the wrinkles of the epidermis, so the electronic can be used to robustly measure biosignals regardless of motion or the topology of the skin. In contrast to conventional electrodes, one triangular patch can be used to record ECG signals without lines and gel, and without glue for adhesion, which enables the long-term, continuous, comfortable, and robust recording of biosignals. The low modulus of CNT/aPDMS means that it can penetrate into the valleys of the skin similar to the gel, which enlarges the contact area and reduces the contact impedance significantly when compared to dry electrodes. Moreover its adhesion force was greatly enhanced compared to other conformal contactable electrode which relies on van der Waals force alone or other adhesives like silicone membranes, spray-on-bandages, Tegaderm films or silicon tapes^{3,31,32}.

This electrode can be used for several times as its adhesion force is restored by cleaning procedure, and multiple peel off test revealed no significant changes in ECG waveform. However, this electrode can easily fracture due to its thinness, and thus should be handled with care. This causes the reusability of the electrodes to be comparatively lower than that of the rigid typed electrodes, especially the capacitive electrodes^{12,33}. However, its mechanical and electrical performance were much better than those of the capacitive electrodes. Moreover, its reusability should not be very low compared to the skin-like electrodes including the capacitive typed electrode³⁴.

This skin-like and self-adhesive electronics also exhibited reduced motion artifacts as CNT/aPDMS was not only penetrated but also adhered even to the grooves to prevent artifact induced by friction as soft elastomer acts like a skin adaptive foam^{2,35}. The robustness with respect to motion artifacts is comparable to that of Ag/AgCl electrodes. This electrode is fully waterproof, which enhances its feasibility and utility for biopotential monitoring in daily life. Even when submerged in water, an ECG can be successfully recorded, which means that the subject can participate in various daily events. This CNT/aPDMS electrode can be attached to various locations of the body, so biosignals such as EOG or EMG can be recorded (Supplementary Fig. S17). Moreover, the terminals of the CNT/aPDMS electrode are solderable, so commercial electric elements can be directly integrated to it, which significantly extends its applications. CNT/aPDMS successfully penetrates the valleys of the skin, so the contact impedance

is significantly reduced compared to that of dry electrodes. Almost 100% of the skin surface to which the CNT/aPDMS electrode is attached in conformal contact with the electrode; since the impedance is inversely proportional to the area, the contact impedance with respect to the skin is minimized. Further, the conductivity of air is very poor (3×10^{-15} to 8×10^{-15} S/m), so the amount of air between the electrode and the skin should be minimized.

In conclusion, the use of CNT/aPDMS as an interfacial layer is a promising strategy for the development of a continuous and inconspicuous health monitoring electronics. This approach combines the advantages of dry electrodes, such as semi-permanency, facility of use, and gel-free use, and those of wet electrodes such as reduced motion artifacts and high signal quality. Moreover, the self-adhesive property of CNT/aPDMS is another big advantage because glue also causes skin trouble. Although many surface electrodes have been developed, their use of gel is a significant obstacle to biomedical applications. The highly conformal adhesive properties of conductive CNT/aPDMS eliminate the need for gel, which means that it can be extensively used in the inconspicuous continuous monitoring of personal health, the early diagnosis of critical diseases and interfacing between human and machine for game, robot control and prosthesis, and diverse mobile and wearable devices, which is one of recent hot issues.

Methods

Human experiments. The study protocol was approved by the Institutional Review Board (IRB) of Korea University, Seoul, South Korea, and all subjects provided written informed consent. The experiments were carried out in accordance with the approved guidelines of IRB.

Fabrication Process. A 4 inch wafer with deposited Au/Ti was prepared before fabrication of the electrode for easy detachment from the Si wafer during final processing. PDMS was spin coated onto the metal-deposited wafer and fully cured in an oven. After treatment with O_2 plasma to prepare a hydrophilic surface, PI (Durimide 7505, Fujifilm Electronic Materials) was spin coated onto the wafer. UV light was irradiated onto the PI layer to define the layout of the substrate, and a Au/Ti metal layer was deposited consecutively with electron beam evaporation then patterned by a wet etching process. Another PI layer was defined as an insulation layer of the electrode, then Ni-plating was performed at the four terminals. After positioning a film shadow mask layer on the resulting electrode for selective casting, uncured CNT/aPDMS was poured and raked out with slide glass for uniform thickness. The shadow mask was removed, then the adhesive CNT/DPMS was fully cured in an oven and aPDMS was injected with a syringe to fill the rest of the area after covering the OHP film on the adhesion side. After curing, the triangular outline was cut with a blade then the electrode was detached from the wafer.

- Lin, C. T. *et al.* Novel Dry Polymer Foam Electrodes for Long-Term EEG Measurement. *Ieee T Bio-Med Eng* **58**, 1200–1207 (2011).
- Chi, Y. M., Jung, T. P. & Cauwenberghs, G. Dry-contact and noncontact biopotential electrodes: methodological review. *IEEE reviews in biomedical engineering* **3**, 106–119 (2010).
- Yeo, W. H. *et al.* Multifunctional Epidermal Electronics Printed Directly Onto the Skin. *Adv Mater* **25**, 2773–2778 (2013).
- Jeong, J. W. *et al.* Materials and Optimized Designs for Human-Machine Interfaces Via Epidermal Electronics. *Adv Mater* **25**, 6839–6846 (2013).
- Jeong, G. S. *et al.* Solderable and electroplatable flexible electronic circuit on a porous stretchable elastomer. *Nat Commun* **3**, 977 (2012).
- Sekitani, T. *et al.* A rubberlike stretchable active matrix using elastic conductors. *Science* **321**, 1468–1472 (2008).
- Webb, R. C. *et al.* Ultrathin conformal devices for precise and continuous thermal characterization of human skin. *Nat Mater* **12**, 938–944 (2013).
- Yamada, T. *et al.* A stretchable carbon nanotube strain sensor for human-motion detection. *Nature nanotechnology* **6**, 296–301 (2011).
- Lipomi, D. J. *et al.* Skin-like pressure and strain sensors based on transparent elastic films of carbon nanotubes. *Nature nanotechnology* **6**, 788–792 (2011).
- Gong, S. *et al.* A wearable and highly sensitive pressure sensor with ultrathin gold nanowires. *Nat Commun* **5**, 3132 (2014).
- Nemati, E., Deen, M. J. & Mondal, T. A Wireless Wearable ECG Sensor for Long-Term Applications. *Ieee Commun Mag* **50**, 36–43 (2012).
- Lee, S. M., Sim, K. S., Kim, K. K., Lim, Y. G. & Park, K. S. Thin and flexible active electrodes with shield for capacitive electrocardiogram measurement. *Med Biol Eng Comput* **48**, 447–457 (2010).
- Miao, M. H. Electrical conductivity of pure carbon nanotube yarns. *Carbon* **49**, 3755–3761 (2011).



14. Han, Z. D. & Fina, A. Thermal conductivity of carbon nanotubes and their polymer nanocomposites: A review. *Prog Polym Sci* **36**, 914–944 (2011).
15. Jung, H. C. *et al.* CNT/PDMS Composite Flexible Dry Electrodes for Long-Term ECG Monitoring. *Ieee T Bio-Med Eng* **59**, 1472–1479 (2012).
16. Xu, F. & Zhu, Y. Highly conductive and stretchable silver nanowire conductors. *Adv Mater* **24**, 5117–5122 (2012).
17. Hu, W. L. *et al.* Intrinsically stretchable transparent electrodes based on silver-nanowire-crosslinked-polyacrylate composites. *Nanotechnology* **23** (2012).
18. Niu, X. Z., Peng, S. L., Liu, L. Y., Wen, W. J. & Sheng, P. Characterizing and patterning of PDMS-based conducting composites. *Adv Mater* **19**, 2682–+ (2007).
19. Zhang, Y. H. *et al.* Buckling in serpentine microstructures and applications in elastomer-supported ultra-stretchable electronics with high areal coverage. *Soft Matter* **9**, 8062–8070 (2013).
20. Bossuyt, F., Vervust, T. & Vanfleteren, J. Stretchable Electronics Technology for Large Area Applications: Fabrication and Mechanical Characterization. *Ieee T Comp Pack Man* **3**, 229–235 (2013).
21. Determan, M. D., Fung, S. S.-O., Filiatrault, T. D., Liu, J. J. & Allen, C. *Gentle to skin adhesive*. *United States patent US20140011021 A1* (2013).
22. Hong, J. S., Lee, J. H. & Nam, Y. W. Dispersion of solvent-wet carbon nanotubes for electrical CNT/polydimethylsiloxane composite. *Carbon* **61**, 577–584 (2013).
23. Lee, S. M. *et al.* A capacitive, biocompatible and adhesive electrode for long-term and cap-free monitoring of EEG signals. *J Neural Eng* **10** (2013).
24. Kwak, M. K., Jeong, H. E. & Suh, K. Y. Rational Design and Enhanced Biocompatibility of a Dry Adhesive Medical Skin Patch. *Adv Mater* **23**, 3949–+ (2011).
25. Schwindt, D. A., Wilhelm, K. P., Miller, D. L. & Maibach, H. I. Cumulative irritation in older and younger skin: a comparison. *Acta Derm-Venereol* **78**, 279–283 (1998).
26. Wang, S. D. *et al.* Mechanics of Epidermal Electronics. *J Appl Mech-T Asme* **79** (2012).
27. Searle, A. & Kirkup, L. A direct comparison of wet, dry and insulating bioelectric recording electrodes. *Physiol Meas* **21**, 271–283 (2000).
28. Oh, T. I. *et al.* Nanofiber Web Textile Dry Electrodes for Long-Term Biopotential Recording. *Ieee T Biomed Circ S* **7**, 204–211 (2013).
29. Baranchuk, A. *et al.* Electrocardiography Pitfalls and Artifacts: The 10 Commandments. *Crit Care Nurse* **29**, 67–73 (2009).
30. Baek, D. H. *et al.* Soldering-based easy packaging of thin polyimide multichannel electrodes for neuro-signal recording. *J Micromech Microeng* **22** (2012).
31. Kim, D. H. *et al.* Epidermal electronics. *Science* **333**, 838–843 (2011).
32. Klode, J. *et al.* Investigation of adhesion of modern wound dressings: a comparative analysis of 56 different wound dressings. *Journal of the European Academy of Dermatology and Venereology : JEADV* **25**, 933–939 (2011).
33. Lim, Y. G., Kim, K. K. & Park, K. S. ECG measurement on a chair without conductive contact. *Ieee T Bio-Med Eng* **53**, 956–959 (2006).
34. Jeong, J. W. *et al.* Capacitive Epidermal Electronics for Electrically Safe, Long-Term Electrophysiological Measurements. *Advanced healthcare materials* (2013).
35. Gruetzmänn, A., Hansen, S. & Müller, J. Novel dry electrodes for ECG monitoring. *Physiol Meas* **28**, 1375–1390 (2007).

Acknowledgments

This study was supported by a grant of the Korea Healthcare technology R&D Project, Ministry for Health, Welfare & Family Affairs, Republic of Korea. (HI09C14060101).

Author contributions

S.M.L. developed the electrode, proposed the key idea of this paper, designed and carried out the experiments, prepared most of the data, and wrote the paper; H.J.B. proposed the idea for the electronics, carried out the soldering experiments and prepared the data; J.H.L. carried out the experiments for the fabrication of electrodes; D.H.B. developed the metal deposition and patterning procedure; K.H.L. assisted with designing the electrode and analyzing material characteristics; J.S.H. proposed the technique of mixing CNTs in aPDMS and assisted in paper-writing; S.H.L. proposed the key idea, managed the research process, and wrote the paper.

Additional information

Supplementary information accompanies this paper at <http://www.nature.com/scientificreports>

Competing financial interests: The authors declare no competing financial interests.

How to cite this article: Lee, S.M. *et al.* Self-adhesive epidermal carbon nanotube electronics for tether-free long-term continuous recording of biosignals. *Sci. Rep.* **4**, 6074; DOI:10.1038/srep06074 (2014).



This work is licensed under a Creative Commons Attribution-NonCommercial-NoDerivs 4.0 International License. The images or other third party material in this article are included in the article's Creative Commons license, unless indicated otherwise in the credit line; if the material is not included under the Creative Commons license, users will need to obtain permission from the license holder in order to reproduce the material. To view a copy of this license, visit <http://creativecommons.org/licenses/by-nc-nd/4.0/>